HHS Public Access

Author manuscript

*Nature*. Author manuscript; available in PMC 2014 April 24.

Published in final edited form as:

*Nature*. 2013 October 24; 502(7472): 575–579. doi:10.1038/nature12572.

# Adrenaline-activated structure of the $\beta_2$-adrenoceptor stabilized by an engineered nanobody

**Aaron M. Ring**[#1,2], **Aashish Manglik**[#1], **Andrew C. Kruse**[#1], **Michael D. Enos**[1,2], **William I. Weis**[1,2], **K. Christopher Garcia**[1,2,3], and **Brian K. Kobilka**[1]

[1]Department of Molecular and Cellular Physiology, Stanford University, Stanford, CA 94305, USA

[2]Department of Structural Biology, Stanford University, Stanford, CA 94305, USA

[3]Howard Hughes Medical Institute, Stanford University School of Medicine, Stanford, CA 94305, USA

[#] These authors contributed equally to this work.

## Abstract

G protein-coupled receptors (GPCRs) are integral membrane proteins that play an essential role in human physiology, yet the molecular processes through which they bind to their endogenous agonists and activate effector proteins remain poorly understood. Thus far, it has not been possible to capture an active-state GPCR bound to its native neurotransmitter. Crystal structures of agonist-bound GPCRs have relied on the use of either exceptionally high-affinity agonists[1,2] or receptor stabilization by mutagenesis[3-5]. Many natural agonists such as adrenaline, which activates the $\beta_2$-adrenoceptor ($\beta_2$AR), bind with relatively low affinity, and they are often chemically unstable. Using directed evolution, we engineered a high-affinity camelid antibody fragment that stabilizes the active state of the $\beta_2$AR, and used this to obtain crystal structures of the activated receptor bound to multiple ligands. Here, we present structures of active-state $\beta_2$AR bound to three chemically distinct agonists: the ultra high-affinity agonist BI167107, the high-affinity catecholamine agonist hydroxybenzyl isoproterenol, and the low-affinity endogenous agonist adrenaline. The crystal structures reveal a highly conserved overall ligand recognition and activation mode despite diverse ligand chemical structures and affinities that range from 100 nM to ~80 pM. The adrenaline-bound receptor structure is overall similar to the others, but shows



Correspondence and requests for materials should be addressed to K.C.G. (kcgarcia@stanford.edu) or B.K.K. (kobilka@stanford.edu)..

**Author Information** Coordinates and structure factors for the $\beta_2$AR-Nb6B9 complexes with ligands BI167107, HBI, and adrenaline are deposited in the Protein Data Bank under accession codes 4LDE, 4LDL, and 4LDO, respectively. Reprints and permission information is available at www.nature.com/reprints. Readers are welcome to comment on the online version of this article at www.nature.com/nature.

**Supplementary Information** is linked to the online version of the paper at www.nature.com/nature.

**Author Contributions** A.M.R. designed and performed yeast display staining and selection experiments, nanobody expression, purification, and characterization on yeast and by SPR. A.M. and A.C.K designed and performed receptor expression, purification, radioligand binding experiments, and crystallography experiments. M.D.E. performed crystallization experiments with adrenaline-bound $\beta_2$AR under the supervision of A.M. and A.C.K. The manuscript was written by A.M.R., A.M., and A.C.K. W.I.W supervised structure refinement. K.C.G. and B.K.K. supervised experiments, and B.K.K. supervised manuscript preparation.

The authors declare no competing financial interests.

substantial rearrangements in extracellular loop three and the extracellular tip of transmembrane helix 6. These structures also reveal a water-mediated hydrogen bond between two conserved tyrosines, which appears to stabilize the active state of the $\beta_2$AR and related GPCRs.

G-protein coupled receptors (GPCRs) relay extracellular signals across a cell membrane via conformational change following binding of an extracellular agonist. GPCR activation by endogenous agonists remains poorly understood due to the paucity of active receptor structures in complex with agonists. While a number of GPCRs have been crystallized in recent years, only the $\beta_2$-adrenoceptor ($\beta_2$AR) and rhodopsin have been crystallized in fully active states[1,6], and in each case structures are available only for complexes with a single agonist. Due to the conformational plasticity and biochemical instability of agonist-bound receptors[7], the few agonist-bound structures of GPCRs solved thus far have relied on either the use of covalent[1] or extremely high affinity agonists[2], crystallographic chaperones to trap active states (a G protein[8] or antibody fragment[9]), or thermostabilizing mutations[3]. The last approach has only yielded structures of agonist-occupied receptor in partially active[3,4] or inactive[5] conformations.

To better understand how diverse agonists can activate a single receptor, we developed a strategy for stabilizing active-state structures of the $\beta_2$AR bound to low affinity agonists including the natural agonist adrenaline. Here, we describe the directed evolution of Nb80, a conformationally-selective single-domain camelid antibody fragment (nanobody) that was used to obtain the first active-state structure of the $\beta_2$AR[9]. Comparison with the structure of $\beta_2$AR in complex with the G protein $G_s$ confirmed that Nb80 stabilizes a physiologically relevant active state[8]. However, the $\beta_2$AR-Nb80 structure was of modest resolution (3.5 Å) and crystals could only be obtained with the high-affinity agonist BI167107; crystallization trials with catecholamine agonists were unsuccessful despite extensive screening. We reasoned that improving the affinity of Nb80 for agonist-bound $\beta_2$AR would decrease receptor conformational heterogeneity and enable crystallization of the receptor bound to low-affinity agonists. However, directed evolution of conformationally-selective GPCR-binding proteins has never been described, likely due to the challenges involved in biochemical manipulation of integral membrane proteins. We used yeast surface display together with a conformationally-specific selection strategy to improve the binding affinity of Nb80 while maintaining its conformational selectivity. The resulting high-affinity variants retain their specificity for the active state of the receptor characteristic of the original Nb80. Using the high-affinity variant Nb6B9, we determined a high-resolution (2.8 Å) active-state structure of the $\beta_2$AR bound to BI167107, and also determined the structures of the $\beta_2$AR bound to two catechol-containing agonists: hydroxybenzyl isoproterenol (HBI) and adrenaline, an endogenous low-affinity agonist of the $\beta_2$AR, at 3.1 Å and 3.2 Å resolution, respectively.

To assess the feasibility of engineering Nb80, we displayed Nb80 on the surface of the yeast strain EBY100 as an amino-terminal fusion to the yeast cell wall protein Aga2p (Fig. 1a). Yeast displaying Nb80 were stained with purified, detergent-solubilized, biotinylated $\beta_2$AR following pre-incubation of receptor with the agonist BI167107 or the inverse agonist carazolol. Nb80-displaying yeast specifically bound to $\beta_2$AR with an overwhelming

preference for agonist-occupied receptor (Fig. 1b), with an $EC_{50}$ of 140 nM (Supplementary Fig. 1a). Next, we constructed a library of Nb80 mutants in which residues at the receptor-binding surface were randomized with conservative substitutions (Supplementary Fig. 2). The library was subjected to six rounds of selection (Fig. 1c). First, the library was positively selected with decreasing concentrations of BI167107-bound $\beta_2$AR. Prior to positive selection in rounds 2-5, the library was negatively selected against binding to inverse agonist-occupied $\beta_2$AR in order to remove variants that had lost conformational specificity. For the final round of selection, we enriched variants with the slowest dissociation rates. Receptor re-binding was blocked by the addition of a large excess of soluble Nb80 following the initial receptor-binding step (Supplementary Fig. 3). This selection strategy resulted in a progressive increase in binding affinity for agonist-occupied receptor without a similar increase in binding to inverse agonist-occupied receptor (Fig. 1d).

Nanobody 6B9 (Nb6B9) was chosen from 23 variants screened from the final round of selection (Supplementary Fig. 4) as it represented one of the highest affinity binders tested, contained mutations that reached consensus among all sequenced clones, and was the most prevalent sequence observed. We expressed and purified Nb6B9 and Nb80, and then used surface plasmon resonance to measure binding kinetics and affinities. Nb6B9 bound to BI167107-occupied $\beta_2$AR with an affinity of 6.4 nM, a near 10-fold improvement over Nb80 (Fig. 1e). This increase in affinity resulted from a 13-fold reduction in the dissociation rate. Competition binding experiments revealed that the $\beta_2$AR bound adrenaline with a high affinity in the presence of 100 nM Nb6B9, which is comparable to the affinity observed in the presence of the G protein $G_s$ (Fig. 1f).

We used the lipidic mesophase method[10] to crystallize complexes of Nb6B9 with $\beta_2$AR bound to three different ligands, shown in Fig. 2a. Crystals grown with $\beta_2$AR bound to the high affinity agonist BI167107 showed strong diffraction, and a structure was obtained to 2.8 Å resolution (Supplementary Table 1). This represents a significant improvement over the previous 3.5 Å structure of $\beta_2$AR bound to the same ligand[9]. This higher resolution structure showed few differences from the Nb80 complex structure (Supplementary Fig. 5). Mutations in Nb6B9 appear to increase shape complementarity to active $\beta_2$AR (Supplementary Fig. 6). Many water molecules were clearly resolved for the first time, particularly in the extracellular region of the receptor (Fig. 2b, c). On the intracellular side of the receptor, a water molecule was found to mediate a hydrogen bond between Tyr326$^{7.53}$ of the NPxxY motif and the highly conserved Tyr219$^{5.58}$ on the intracellular side of transmembrane helix 5 (TM5), similar to a water seen in a recent structure of metarhodopsin II[11]. Electron density suggestive of a water molecule was also seen in HBI- and adrenaline-bound $\beta_2$AR structures, despite their slightly lower resolution. The water-mediated hydrogen bond between Tyr219$^{5.58}$ and Tyr326$^{7.53}$ is possible only in the active conformation of the receptor (Fig. 2c), and the observed water-mediated hydrogen bond may therefore contribute to active state stability in the $\beta_2$AR and other GPCRs, serving as an active-state counterpart to the “ionic lock” which stabilizes the inactive state[12]. In support of this notion, mutation of the corresponding Tyr223$^{5.58}$ to phenylalanine in rhodopsin decreases the stability of the meta II state[13] and greatly reduces activation of transducin[14]. Moreover, mutation of Tyr227$^{5.58}$ to alanine resulted in the largest increase in thermostability for the inactive-state thermostabilized $\beta_1$AR[15].

While BI167107 exhibits many features typical of $\beta_2$AR agonists, it lacks the catechol moiety of the endogenous agonists adrenaline and noradrenaline. Hence, it is conceivable that these agonists stabilize a different conformation of the activated receptor-binding pocket. To assess this possibility, we pursued crystallographic study of complexes of Nb6B9 with $\beta_2$AR bound to the low-affinity endogenous agonist adrenaline and the high-affinity catecholamine agonist hydroxybenzyl isoproterenol (HBI). In each case, crystals could be grown in nearly identical conditions to those for the BI167107 complex, with clear electron density to identify the position and orientation of each ligand (Supplementary Fig. 7).

Despite the chemical diversity of these ligands, the structures of $\beta_2$AR bound to the catecholamine agonists and BI167107 show highly similar overall structures (Fig. 3a, b). A notable exception is a shift in the position of Asn293$^{6.55}$, which was previously determined to hydrogen bond with the amide carbonyl on the head-group of BI167107. The smaller catechol ring of adrenaline and HBI precludes hydrogen bonding with Asn293$^{6.55}$ in the receptor conformation observed in the BI167107-bound structure. In order to maintain the corresponding hydrogen bond between Asn293 and the *meta* hydroxyl moiety on the catechol ring, the receptor undergoes a 1.2 Å shift in the extracellular side of TM6, which bends toward the ligand (Fig. 3c). This shift alters the hydrogen-bonding network in this region and thereby causes a change in the conformation of His296$^{6.58}$. For adrenaline-bound $\beta_2$AR, the TM6 conformational change is further propagated towards the extracellular side of the receptor, leading to a conformational rearrangement in extracellular loop 3 (Fig. 3d). This change also alters the extracellular surface of the receptor, with adrenaline-bound $\beta_2$AR having a contracted extracellular vestibule (Supplementary Fig. 8).

The relatively subtle differences in receptor conformation observed for the different co-crystallized agonists suggest that the activation mechanism of the $\beta_2$AR is highly similar for all agonists. Much like BI167107, the catechol headgroups of adrenaline and HBI engage $\beta_2$AR residues previously characterized to be important for agonist binding and receptor activation (Supplementary Fig. 9). Consistent with prior mutagenesis studies, Ser203$^{5.42}$ and Ser207$^{5.46}$ make hydrogen bonds with the catecholamine phenoxy moieties[16] (Fig. 3a - c), and the conformation of these residues is nearly identical to that observed for the BI167107 headgroup. Ser204$^{5.43}$, which was previously thought to directly contact the para-hydroxy group of the catecholamine[16,17], engages the catecholamine headgroup indirectly in an extended polar network with Tyr308$^{7.35}$ and Asn293$^{6.55}$. Unlike BI167107-bound $\beta_2$AR, however, this polar interaction network is extended by inclusion of His296$^{6.58}$ in the catecholamine-bound receptor, suggesting that conformational rearrangement of His296$^{6.58}$ may stabilize the slightly smaller orthosteric binding pocket observed for catecholamine agonists. The agonist-induced rearrangements in the central portion of the transmembrane segments and intracellular surface are virtually identical in all three agonist-bound structures (Fig. 3b, Supplementary Fig. 10). Structures of $\beta_2$AR bound to BI167107 and the catecholamine agonists all show highly similar activation-related changes in the residues that connect the orthosteric ligand-binding pocket to the intracellular surface, suggesting that the mechanism for allosteric coupling between the orthosteric binding site and the G-protein coupling domain is likely a conserved feature of $\beta_2$AR activation. Therefore, different

agonists stabilize the same conformational rearrangements in the receptor through different chemical interactions.

In contrast to the striking similarity in receptor conformation for all three agonists crystallized here, far more substantial conformational differences are seen relative to a previously reported structure of the thermostabilized turkey $\beta_1$ adrenoceptor ($\beta_1$AR) bound to the catecholamine agonist isoproterenol[5]. Likely due to the thermostabilization procedure, the overall receptor conformation of isoprenaline-bound $\beta_1$AR closely resembles that of the antagonist-bound, inactive $\beta_1$AR[18], as well as that of covalent agonist-bound, inactive $\beta_2$AR[1] (Supplementary Fig. 11). Thus, a comparison of the structural changes between inactive $\beta_1$AR and active $\beta_2$AR, each bound to catecholamines, offers new insight into how agonists bind adrenoceptors both in the low-affinity state and the high-affinity, G protein-coupled state. Within the binding pocket, isoprenaline makes a hydrogen bond with Ser211$^{5.42}$ and the β-hydroxylamine moiety engages conserved residues Asp$^{3.32}$ and Asn$^{7.39}$ in a highly similar manner to the active state structures (Fig 4a, b). Similar interactions can occur in both active and inactive states, likely accounting for the fact that the β-hydroxylamine moiety is an important feature of both β-adrenoceptor agonists and antagonists/inverse agonists. However, the isoprenaline catechol headgroup engages a limited network of polar contacts in the inactive $\beta_1$AR structure, while adrenaline bound to active $\beta_2$AR engages an extensive polar network linking the orthosteric site to the extracellular loops (Fig. 4a). As a consequence of structural changes stabilized by this polar network, the catechol headgroup of adrenaline is nearly completely enclosed within the orthosteric binding pocket of activated $\beta_2$AR (Fig. 4c). In comparison, isoprenaline bound to inactive $\beta_1$AR is highly exposed to the extracellular solvent and is slightly displaced towards the extracellular side of the receptor (Fig. 4d). Thus, for the β adrenoceptors, the combination of a more extensive polar network and a smaller binding pocket likely accounts for the enhanced agonist affinity in the presence of either $G_s$ or G protein mimetic nanobodies. Moreover, such differences between active and inactive structures highlight the importance of active-state GPCR crystal structures in understanding the structural basis for agonist activity.

In conclusion, the use of new approaches in combinatorial biology has led to the development of Nb6B9, an exceptionally high-affinity GPCR-stabilizing nanobody. This molecule exhibits enhanced affinity for $\beta_2$AR relative to wild-type Nb80, and it allowed crystallization of $\beta_2$AR in complex with three different agonists with diverse chemical structures and a wide range of affinities. The use of such high-affinity crystallization chaperones may be generally useful in determination of active-state structures of GPCRs bound to low-affinity agonists. The crystallographic studies presented here reveal subtle, ligand-specific differences in receptor conformation superimposed on the backdrop of an overall conserved agonist binding mode and activation mechanism, offering new insight into how chemically diverse agonists can activate a single receptor.

# ONLINE METHODS

## $\beta_2$-adrenergic receptor expression and purification

Human $\beta_2$AR bearing an amino-terminal FLAG epitope tag and truncated after residue 365 was expressed in *Sf9* insect cells using the BestBac baculovirus system (Expression Systems; Davis, CA). Cells were infected at a density of $4 \times 10^6$ cells/mL, then incubated for two days at 27 °C. Receptor was extracted as described previously[19]. Receptor was first purified by FLAG affinity chromatography, then labeled with a 10-fold molar excess of biotin-$PEG_{11}$-maleimide (Thermo Scientific; Rockford, IL), which reacts with the endogenous residue Cys265. Following a one-hour incubation at room temperature, unlabeled receptor was blocked with 2 mM iodoacetamide for 15 minutes and then purified by alprenolol sepharose chromatography to isolate only functional receptor. Alprenolol sepharose eluate was concentrated on FLAG affinity resin, and then washed with ligand-free buffer for 30 minutes at room temperature to eliminate bound alprenolol. Detergent was gradually exchanged from dodecyl maltoside (DDM) to lauryl maltose neopentyl glycol (MNG) by washing in buffer containing decreasing amounts of DDM and MNG at a fixed concentration of 0.1% (w/w). Receptor was eluted, aliquoted, and frozen in 20% glycerol.

## Display and functional evaluation of Nb80 on yeast

Nb80 was cloned into the carboxy-terminal Aga2 yeast-display vector pYAL[20] and transformed and displayed on yeast as previously described[21]. Induced yeast displaying Nb80 were washed with PBE buffer (phosphate buffered saline with 0.5 mM EDTA and 0.5% BSA) supplemented with 0.02% MNG detergent (PBEM buffer) and stained with varying concentrations of biotinylated receptor bound to either BI167107 or carazolol for one hour at 4°C. The yeast were then washed with PBEM buffer and stained with Alexa 647-conjugated streptavidin for 15 minutes at 4°C. Mean cell fluorescence was measured using the FL-4 channel of an Accuri C6 flow cytometer.

## Affinity maturation of Nb80

The affinity maturation library was prepared by assembly PCR with oligonucleotide primers (Supplementary Table 3) containing degenerate codons at 15 distinct positions (Supplementary Fig. 2). The PCR product was further amplified with primers containing 50 basepairs of homology to pYal. Mutagenic nanobody DNA and linearized pYAL vector were co-electroporated into EBY100 yeast to yield a library of $0.8 \times 10^8$ transformants.

For the first round of selection, $1.0 \times 10^9$ yeast induced with SGCAA medium were washed with PBEM buffer and then resuspended in 5 mL of PBEM buffer containing 200 nM biotinylated $\beta_2$AR bound to BI167107. After one hour of incubation at 4 °C with rotation, yeast were washed with PBEM buffer, and then stained with Alexa647-conjugated streptavidin in PBEM buffer for 15 minutes at 4°C. Yeast were washed again with PBEM buffer and magnetically labeled with 250 μL anti-647 microbeads (Miltenyi) in 4.75 mL PBEM buffer for 15 minutes at 4°C. Yeast were washed a final time and labeled yeast were isolated by magnetic selection with an LS column (Miltenyi) pre-equilibrated with PBEM buffer. Magnetically-sorted yeast were resuspended in SDCAA medium and cultured at 30°C.

Rounds 2 – 6 were selected in a similar manner, with the following modifications. Prior to positive selection with agonist-occupied $\beta_2$AR, negative selection with antagonist-bound receptor was performed to select for clones that maintained a preference for the active state of the $\beta_2$AR. Briefly, $1.0 \times 10^8$ yeast were washed with PBEM buffer and resuspended in 500 μL PBEM buffer containing 1 μM biotinylated $\beta_2$AR bound to carazolol. Yeast were incubated at 4 °C for one hour, then labeled with Alexa647 or PE-conjugated streptavidin, and magnetically labeled with 50 μL of the respective anti-fluorophore microbeads (Miltenyi) in 450 μL PBEM buffer. Magnetically-labeled yeast were applied to an LS column and the depleted flow-through was collected for subsequent positive selection. In this manner, yeast clones binding the 'inactive,' antagonist-occupied receptor were discarded. Positive selections on 'active,' agonist-occupied receptor were performed as for round one, but in a staining volume of 500 μL and with successively decreasing concentrations of BI167107-bound $\beta_2$AR: 200 nM receptor for rounds 2 and 3, 20 nM receptor for round 4, and 1 nM receptor for round 5. For round 6, positive selection was performed by a kinetic selection strategy to select for clones with the slowest off-rates (Supplementary Fig. 3). Briefly, yeast were stained with 200 nM biotinylated BI167107-bound $\beta_2$AR for one hour, washed with PBEM, and then resuspended in 500 μL PBEM containing 15 μM Nb80. The cells were incubated at 25 °C for 155 minutes, after which they were washed with ice-cold PBEM and stained with fluorescent streptavidin. Enrichment with magnetic separation for rounds 2 – 6 was performed as for round one, but with 50 μL anti-fluorophore magnetic microbeads with 450 μL PBEM buffer. Subsequent to round 6, post-sorted yeast were plated onto SDCAA-agar plates, colonies were picked and cultured in liquid SDCAA medium, and the plasmids encoding the nanobodies were isolated with a ZymoPrep Yeast Plasmid Miniprep II kit (Zymo Research) and sequenced.

## Expression and characterization of Nb80 and Nb6B9

Nanobodies were cloned into the periplasmic expression vector pET26b, containing an amino terminal signal sequence and a carboxy-terminal 8×histidine tag and transformed into BL21(DE3) Rosetta2 *E. coli* (Novagen). Cells were induced in Terrific Broth at an $OD_{600}$ of 0.8 with 1 mM IPTG and incubated with shaking at 22 °C for 24 hours. Periplasmic protein was obtained by osmotic shock and the nanobodies were purified using nickel–nitrilotriacetic acid (Ni-NTA) chromatography[9]. For crystallography, Nb6B9 was digested overnight with 1:50 (w/w) carboxypeptidase A (Sigma) to remove the His tag, then purified by size exclusion chromatography over a Sephadex S200 size exclusion column.

Surface plasmon resonance experiments were conducted with a Biacore T100 at 25 °C. Protein concentrations were determined by 280 nm absorbance with a Nanodrop2000 spectrometer (Thermo Scientific). Biotinylated BI167107-bound $\beta_2$AR was immobilized on an SA sensorchip (GE) at an $R_{max}$ of approximately 40 response units (RU). Biotinylated tiotropium-bound $M_2$ muscarinic receptor was immobilized with an RU value matching that of the reference surface to control for nonspecific binding. Measurements were made using serial dilutions of Nb80 or Nb6B9 in HBSM (10 mM HEPES pH 7.4, 150 mM NaCl, 0.01% MNG) using single-cycle kinetics. All data were analyzed with the Biacore T100 evaluation software version 2.0 with a 1:1 Langmuir binding model.

Radioligand binding assays were performed using purified $\beta_2$AR reconstituted into HDL particles comprised of apolipoprotein A1 and a 3:2 (mol:mol) mixture of POPC:POPG lipid[22]. Binding experiments with G-protein were performed as previously described[8]. Binding reactions were 500 μL in volume, and contained 50 fmol functional receptor, 0.5 nM $^3$H dihydroalprenolol ($^3$H-DHA), 100 mM NaCl, 20 mM HEPES pH 7.5, 0.1% bovine serum albumin, and ligands and nanobodies as indicated. Reactions were mixed, then incubated for four hours at room temperature prior to filtration with a Brandel 48-well harvester onto a filter pre-treated with 0.1% polyethylenimine. Radioactivity was measured by liquid scintillation counting. All measurements were performed in triplicate, and are presented as means ± SEM.

### Purification and crystallization of $\beta_2$AR-Nb6B9 complexes

Human $\beta_2$AR fused to an amino-terminal T4 lysozyme[23] was expressed and purified as described above. Following purification by alprenolol sepharose, the receptor was washed extensively with 30 μM of the low affinity antagonist atenolol while bound to FLAG affinity resin to fully displace alprenolol, then washed and eluted in buffer devoid of ligand to produce a homogeneously unliganded preparation. The receptor was then incubated for 30 minutes at room temperature with a stoichiometric excess of ligand (HBI or BI167107). A 1.3-fold molar excess of Nb6B9 was then added, and the sample was dialyzed overnight into a buffer consisting of 100 mM sodium chloride, 20 mM HEPES pH 7.5, 0.01% lauryl maltose neopentyl glycol detergent, and 0.001% cholesteryl hemisuccinate. In each case, ligand was included in the dialysis buffer at 100 nM concentration or higher. The sample was then concentrated using a 50 kDa spin concentrator and purified over a Sephadex S200 size exclusion column in the same buffer as for dialysis, and the $\beta_2$AR-Nb6B9-ligand ternary complex was isolated. In the case of adrenaline, the low affinity and chemical instability of the ligand precluded overnight dialysis, so 100 μM adrenaline was added to receptor for 30 minutes at room temperature, then a 1.3-fold molar excess of Nb6B9 added and the sample was incubated for 30 minutes at room temperature. Following incubation, the sample was concentrated and immediately purified by size exclusion as above.

Following purification, samples were concentrated to $A_{280}$ = 55 using a 50 kDa concentrator to minimize the detergent concentration in the final sample, then aliquoted into thin-walled PCR tubes at 8 μL per aliquot. Aliquots were flash frozen in liquid nitrogen and stored at -80 °C for crystallization trials. For crystallization, samples were thawed and reconstituted into lipidic cubic phase with a 1:1 mass:mass ratio of lipid. The lipid stock consisted of a 10:1 mix by mass of 7.7 monoacylglycerol (generously provided by Martin Caffrey) with cholesterol (Sigma). Samples were reconstituted by the two syringe mixing method[10] and then dispensed into glass sandwich plates using a GryphonLCP robot (Art Robbins Instruments). In the case of the $\beta_2$AR-adrenaline complex, 1 mM fresh adrenaline was mixed with receptor prior to reconstitution. Crystals were grown using 30 nL protein/lipid drops with 600 nL overlay solution, which consisted of 18 – 24 % PEG400, 100 mM MES pH 6.2 to pH 6.7, and 40 – 100 mM ammonium phosphate dibasic. Crystals grew in 1 – 3 days, and were harvested and frozen in liquid nitrogen for data collection.

### Crystallographic data collection and refinement

X-ray diffraction data were collected at Advanced Photon Source GM/CA beamlines 23ID-B and 23ID-D. The best diffracting crystals were identified by rastering, and wedges of 1–10° were collected using a 10 μm beam with typically 2 seconds exposure, 0.6° oscillation, and no beam attenuation. Data collection statistics are summarized in Supplementary table 1. Diffraction data were processed in *HKL2000*[24], and the structure was solved using molecular replacement with the structures of active $\beta_2$AR, Nb80 (PDB ID: 3P0G), and T4 lysozyme (PDB ID: 2RH1) used as search models in *Phaser*[25]. The resulting structure was iteratively refined in *Phenix*[26] and manually rebuilt in *Coot*[27]. Final refinement statistics are summarized in Supplementary table 1. Figures were prepared in *PyMol*.

## Supplementary Material

Refer to Web version on PubMed Central for supplementary material.

## Acknowledgements

We thank Daniel Hilger for critical reading of the manuscript. We acknowledge support from the Stanford Medical Scientist Training Program (A.M. and A.M.R.), the American Heart Association (A.M.), the National Science Foundation (A.C.K.), the Ruth L. Kirschstein National Research Service Award (A.M.R.), NIH grants NS02847123 and GM08311806 (B.K.K.), from the Mathers Foundation (B.K.K., W.I.W., and K.C.G), and from the Howard Hughes Medical Institute (K.C.G.).

## References

1. Rosenbaum DM, et al. Structure and function of an irreversible agonist-beta(2) adrenoceptor complex. Nature. 2011; 469:236–240. doi:10.1038/nature09665. [PubMed: 21228876]
2. Xu F, et al. Structure of an agonist-bound human A2A adenosine receptor. Science. 2011; 332:322–327. doi:10.1126/science.1202793. [PubMed: 21393508]
3. White JF, et al. Structure of the agonist-bound neurotensin receptor. Nature. 2012; 490:508–513. doi:10.1038/nature11558. [PubMed: 23051748]
4. Lebon G, et al. Agonist-bound adenosine A2A receptor structures reveal common features of GPCR activation. Nature. 2011; 474:521–525. doi:10.1038/nature10136. [PubMed: 21593763]
5. Warne T, et al. The structural basis for agonist and partial agonist action on a beta(1)-adrenergic receptor. Nature. 2011; 469:241–244. doi:10.1038/nature09746. [PubMed: 21228877]
6. Venkatakrishnan AJ, et al. Molecular signatures of G-protein-coupled receptors. Nature. 2013; 494:185–194. doi:10.1038/nature11896. [PubMed: 23407534]
7. Nygaard R, et al. The dynamic process of beta(2)-adrenergic receptor activation. Cell. 2013; 152:532–542. doi:10.1016/j.cell.2013.01.008. [PubMed: 23374348]
8. Rasmussen SG, et al. Crystal structure of the beta2 adrenergic receptor-Gs protein complex. Nature. 2011; 477:549–555. doi:10.1038/nature10361. [PubMed: 21772288]
9. Rasmussen SG, et al. Structure of a nanobody-stabilized active state of the beta(2) adrenoceptor. Nature. 2011; 469:175–180. doi:10.1038/nature09648. [PubMed: 21228869]
10. Caffrey M, Cherezov V. Crystallizing membrane proteins using lipidic mesophases. Nat. Protocols. 2009; 4:706–731. [PubMed: 19390528]
11. Deupi X, et al. Stabilized G protein binding site in the structure of constitutively active metarhodopsin-II. Proc Natl Acad Sci U S A. 2012; 109:119–124. doi:10.1073/pnas.1114089108. [PubMed: 22198838]
12. Schneider EH, Schnell D, Strasser A, Dove S, Seifert R. Impact of the DRY motif and the missing “ionic lock” on constitutive activity and G-protein coupling of the human histamine H4 receptor. J Pharmacol Exp Ther. 2010; 333:382–392. doi:10.1124/jpet.109.163220. [PubMed: 20106995]

13. Elgeti M, et al. Conserved Tyr223(5.58) plays different roles in the activation and G-protein interaction of rhodopsin. J Am Chem Soc. 2011; 133:7159–7165. doi:10.1021/ja200545n. [PubMed: 21506561]
14. Goncalves JA, et al. Highly conserved tyrosine stabilizes the active state of rhodopsin. Proc Natl Acad Sci U S A. 2010; 107:19861–19866. doi:10.1073/pnas.1009405107. [PubMed: 21041664]
15. Serrano-Vega MJ, Magnani F, Shibata Y, Tate CG. Conformational thermostabilization of the beta1-adrenergic receptor in a detergent-resistant form. Proc Natl Acad Sci U S A. 2008; 105:877–882. doi:10.1073/pnas.0711253105. [PubMed: 18192400]
16. Strader CD, Candelore MR, Hill WS, Sigal IS, Dixon RA. Identification of two serine residues involved in agonist activation of the beta-adrenergic receptor. J Biol Chem. 1989; 264:13572–13578. [PubMed: 2547766]
17. Liapakis G, et al. The forgotten serine. A critical role for Ser-2035.42 in ligand binding to and activation of the beta 2-adrenergic receptor. J Biol Chem. 2000; 275:37779–37788. doi:10.1074/jbc.M002092200. [PubMed: 10964911]
18. Warne T, et al. Structure of a beta1-adrenergic G-protein-coupled receptor. Nature. 2008; 454:486–491. doi:10.1038/nature07101. [PubMed: 18594507]
19. Kobilka BK. Amino and Carboxyl Terminal Modifications to Facilitate the Production and Purification of a G Protein-Coupled Receptor. Analytical Biochemistry. 1995; 231:269–271. doi:10.1006/abio.1995.1533. [PubMed: 8678314]
20. Wang Z, Mathias A, Stavrou S, Neville DM Jr. A new yeast display vector permitting free scFv amino termini can augment ligand binding affinities. Protein Eng Des Sel. 2005; 18:337–343. doi:10.1093/protein/gzi036. [PubMed: 15976011]
21. Chao G, et al. Isolating and engineering human antibodies using yeast surface display. Nat Protoc. 2006; 1:755–768. doi:10.1038/nprot.2006.94. [PubMed: 17406305]
22. Whorton MR, et al. A monomeric G protein-coupled receptor isolated in a high-density lipoprotein particle efficiently activates its G protein. Proc Natl Acad Sci U S A. 2007; 104:7682–7687. doi:10.1073/pnas.0611448104. [PubMed: 17452637]
23. Zou Y, Weis WI, Kobilka BK. N-terminal T4 lysozyme fusion facilitates crystallization of a G protein coupled receptor. PLoS One. 2012; 7:e46039. doi:10.1371/journal.pone.0046039. [PubMed: 23056231]
24. Otwinowski, Z.; Minor, W. Methods in Enzymology. Carter, Charles W., Jr., editor. Vol. Vol. Volume 276. Academic Press; 1997. p. 307-326.
25. McCoy AJ, et al. Phaser crystallographic software. J Appl Crystallogr. 2007; 40:658–674. doi:10.1107/s0021889807021206. [PubMed: 19461840]
26. Afonine PV, et al. Towards automated crystallographic structure refinement with phenix.refine. Acta Crystallogr D Biol Crystallogr. 2012; 68:352–367. doi:10.1107/s0907444912001308. [PubMed: 22505256]
27. Emsley P, Cowtan K. Coot: model-building tools for molecular graphics. Acta Crystallogr D Biol Crystallogr. 2004; 60:2126–2132. doi:10.1107/s0907444904019158. [PubMed: 15572765]

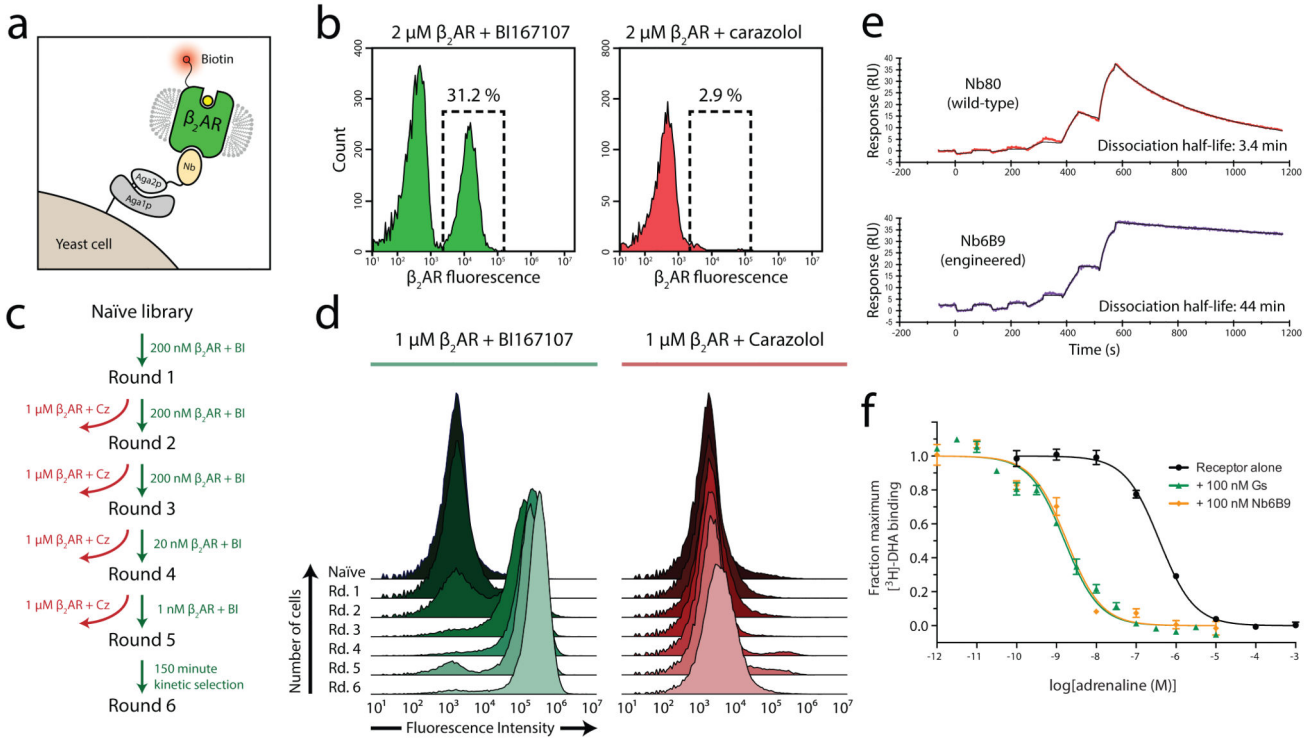


**Figure 1. Conformational selection of nanobodies and characterization of high affinity Nb6B9**

**a,** Schematic representation of yeast display of Nb80. Nb80 is fused to the amino terminus of Aga2p, which attaches to the yeast cell wall through a covalent interaction with Aga1p. **b,** Staining of Nb80-expressing yeast with $\beta_2$AR bound to the agonist BI167107 (left) or the inverse agonist carazolol (right). **c,** Flow-chart summary of conformational selection process. **d,** Histogram overlays assessing $\beta_2$AR staining of the library at each round of selection. The left panel shows staining with 1 μM BI167107-occupied receptor, while the right panel shows staining with 1 μM carazolol-occupied receptor. **e,** Representative single-cycle kinetics SPR sensorgram of wild-type Nb80 (top) and engineered Nb6B9 binding immobilized $\beta_2$AR bound to BI167107. **f,** $^3$H-dihydroalprenolol ($^3$H-DHA) competition binding shows a comparable increase in $\beta_2$AR affinity for adrenaline in the presence of Nb6B9 as with G protein $G_s$. $^3$HDHA affinity is largely unchanged in the presence of Nb6B9 (Supplementary Table 2). Data and error bars represent the mean ± standard error of the mean from three experiments.

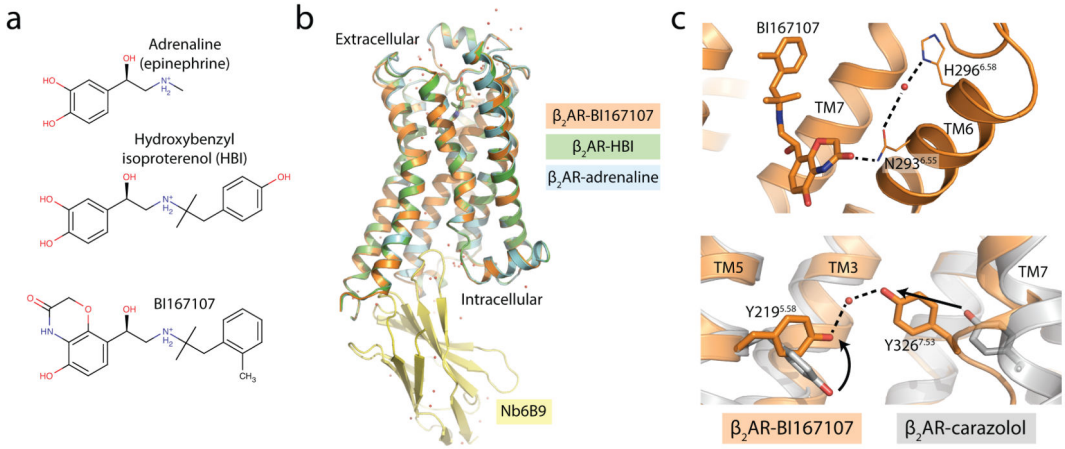


**Figure 2. Structure of the activated $\beta_2$AR in complex with three agonists**

**a,** Chemical structures of the three ligands used for crystallization trials. **b,** All three active-state structures, showing remarkable similarity in overall receptor conformation. **c,** The 2.8 Å resolution structure of BI167107-bound $\beta_2$AR reveals active-state water molecules: a bridging water molecule participates in a polar network at the ligand binding site (top) and a second water molecule mediates a hydrogen bond between two highly conserved tyrosines. Such an interaction is possible in the active state (orange) but not the inactive state (gray).

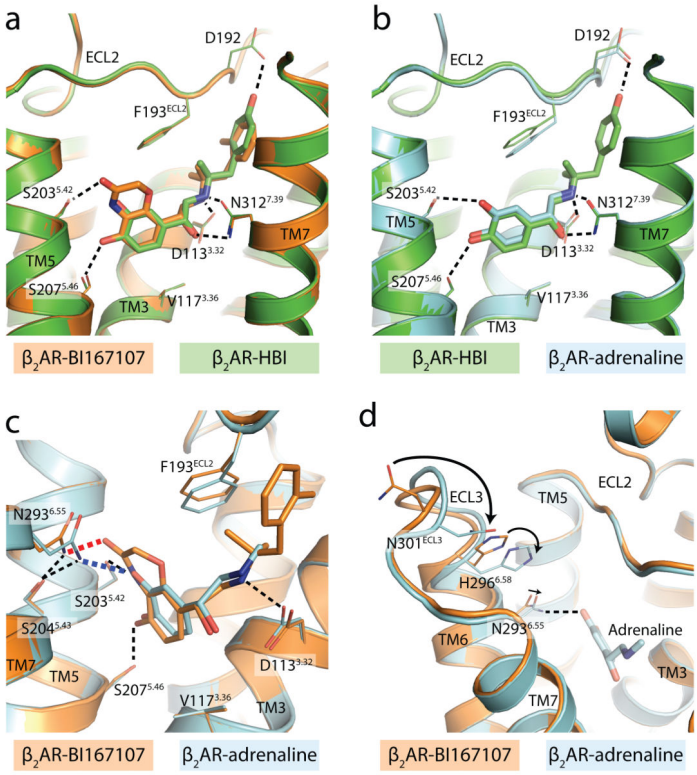


**Figure 3. Comparison of agonist binding modes**

**a,** Comparison of BI167107-bound receptor (orange) with HBI-bound receptor (green) shows highly conserved agonist binding mode. **b,** Similarly, adrenaline-bound (cyan) and HBI-bound (green) receptor structures are highly similar. **c**, An analogous comparison of BI167107-bound $\beta_2$AR (orange) with adrenaline-bound receptor (cyan) shows the similar polar networks for the two ligands (black dotted lines) with a notable difference in the hydrogen bonding of Asn293$^{6.55}$ to the amide proton in BI167107 (red dotted line) or the *meta* hydroxyl of adrenaline (blue dotted line) **d,** Due to this difference, Asn293$^{6.55}$ and TM6 shift inward in the adrenaline-bound structure,, leading to a cascade of changes culminating in a rearrangement of ECL3.

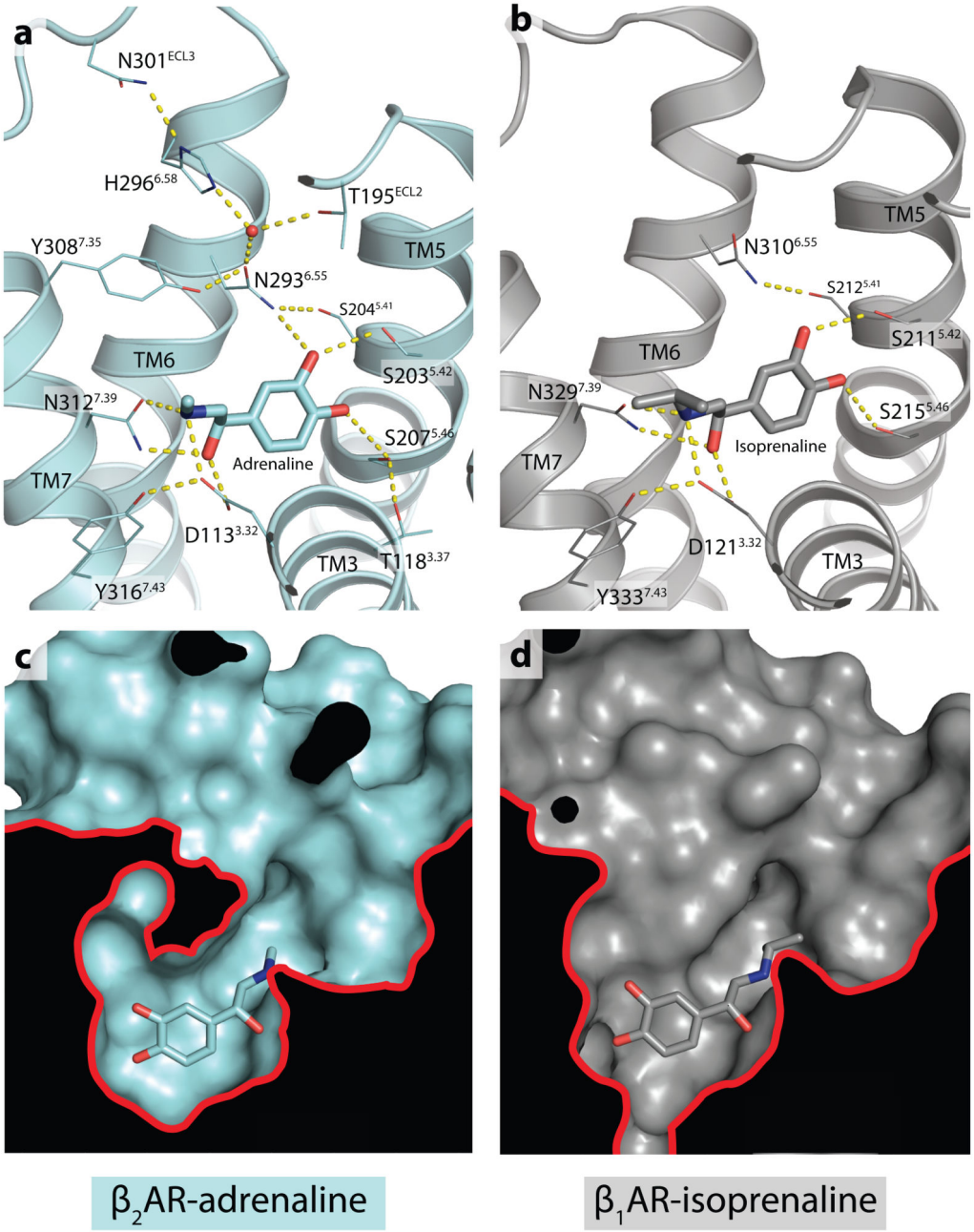


**Figure 4. Activation by catecholamine agonists**

For the first time, structures of catecholamine-bound adrenergic receptors in active and inactive conformations can be compared. **a,** The structure of $\beta_2$AR in an active conformation bound to the agonist adrenaline reveals an extended polar contact network linking the orthosteric site to extracellular loops 2 and 3, while the structure of thermostabilized $\beta_1$AR in an inactive conformation bound to a similar catecholamine agonist, isoprenaline, shows a far more limited polar network. **c,** Likewise, a surface view of the active state structure

shows a substantial contraction of the binding site compared with **d,** the inactive $\beta_1$AR structure.